Phenology of marine phytoplankton from satellite ocean color measurements

M. Vargas,[1] C. W. Brown,[1,2] and M. R. P. Sapiano[2]

[1] Climate change is expected to affect the timing and magnitude of numerous environmental conditions, including temperature, wind, and precipitation. Amongst other repercussions, such alterations will engender a response in marine ecosystem productivity manifested by changes in the timing and magnitude of phytoplankton biomass and primary productivity. Several investigations have examined the change in magnitude in chlorophyll concentration in relation to changing environmental conditions, but little has been done to examine the change in the timing of the annual cycle of phytoplankton biomass. In order to establish a baseline from which to assess any future changes in the phenology of phytoplankton biomass, we constructed nine-year climatologies of phytoplankton bloom onset, maturity, start of bloom decay, and termination in the central North Atlantic. This was accomplished by extracting annual values of these phenological markers from Generalized Linear Models fit to pentad (five-day) estimates of SeaWiFS chlorophyll concentrations dating from 1998 to 2006. This novel modeling approach, which produced results consistent with known patterns of phytoplankton bloom dynamics in this region, provides a statistically robust approach to detect and account for changes in the annual cycle of phytoplankton biomass. **Citation:** Vargas, M., C. W. Brown, and M. R. P. Sapiano (2009), Phenology of marine phytoplankton from satellite ocean color measurements, *Geophys. Res. Lett.*, *36*, L01608, doi:10.1029/2008GL036006.

1. Introduction

[2] Phytoplankton standing stocks and productivity exhibit variability in the timing and magnitude within different regions of the ocean because processes affecting their growth and demise, such as incident solar irradiance, water column stratification, nutrient supply, and grazing pressure, vary with latitude and oceanographic conditions [*Cushing*, 1959; *Yoder et al.*, 1993]. Climate change will affect many of these oceanic conditions and will thus affect the timing and magnitude of primary production with important consequences for aquatic life and the ocean carbon cycle [*Edwards and Richardson*, 2004; *Hays et al.*, 2005; *Stenseth and Mysterud*, 2002]. Warmer ocean temperatures, for example, increase stratification of the surface mixed layer, inhibiting the entrainment of nutrients from below that support primary production [*Sarmiento et al.*, 2004].

[3] Satellites provide the routine, synoptic measurements to document these potential changes in phytoplankton biomass and productivity on basin to global scales. Though several investigations using satellite measurements have examined the variability in the magnitude in chlorophyll concentration (a proxy for phytoplankton biomass) in relation to changing environmental conditions [*Behrenfeld et al.*, 2001, 2006; *Gregg and Conkright*, 2002; *Gregg et al.*, 2003], little has been done to investigate the variability in the timing of primary productivity and phytoplankton biomass. On land, the timing of seasonal flowering and greening of vegetation has advanced [*Beaubien and Hall-Beyer*, 2003; *Delbart et al.*, 2006; *Schwartz*, 1999; *Zhang et al.*, 2006] and the active growing season in the Northern hemisphere from 1981 to 1991 has lengthened [*Myneni et al.*, 1997]. Our primary interest is in determining whether a similar response is occurring in the oceans.

[4] The few satellite studies that have examined phenological characteristics of the annual cycle of phytoplankton biomass have principally investigated bloom initiation or peak and were regionally limited, with the majority focusing on the North Atlantic [e.g., *Henson et al.*, 2006; *Henson and Thomas*, 2007; *Siegel et al.*, 2002; *Ueyama and Monger*, 2005]. *Siegel et al.* [2002] used a three-year time series of SeaWiFS chlorophyll concentration to study the spatial distribution of bloom onset in the North Atlantic and showed that blooms start in winter south of 40°N whereas they start in the spring north of 50°N. *Ueyama and Monger* [2005] determined the timing and magnitude of seasonal phytoplankton blooms in the North Atlantic by analyzing a least-squares fit curve of a seven-year time series of SeaWiFS chlorophyll and reported that blooms occurred between autumn and winter in subtropical regions (<40°N) and during spring at subpolar and polar latitudes (>40°N). Beyond bloom onset, the documentation and variability of other stages or phenological markers are largely unknown. Some investigators calculated bloom duration, often defined as the difference in time between bloom onset and termination [*Platt et al.*, 2003; *Ueyama and Monger*, 2005], but it has not been thoroughly described. Documenting additional phenological markers may lead to a better understanding of the processes affecting phytoplankton and help monitor the response of phytoplankton to environmental change.

2. Methodology

[5] Pentad (five-day mean) estimates of chlorophyll concentrations dating from 1 January 1998 to 31 December 2006 with a spatial resolution of 3° × 3° were generated from daily, 1/12° SeaWiFS chlorophyll concentrations over the central North Atlantic (42°N–15°N, 60°W–21°W; Figure 1). These daily chlorophyll fields were produced

---

[1]Center for Satellite Applications and Research, National Oceanic and Atmospheric Administration, Camp Springs, Maryland, USA.

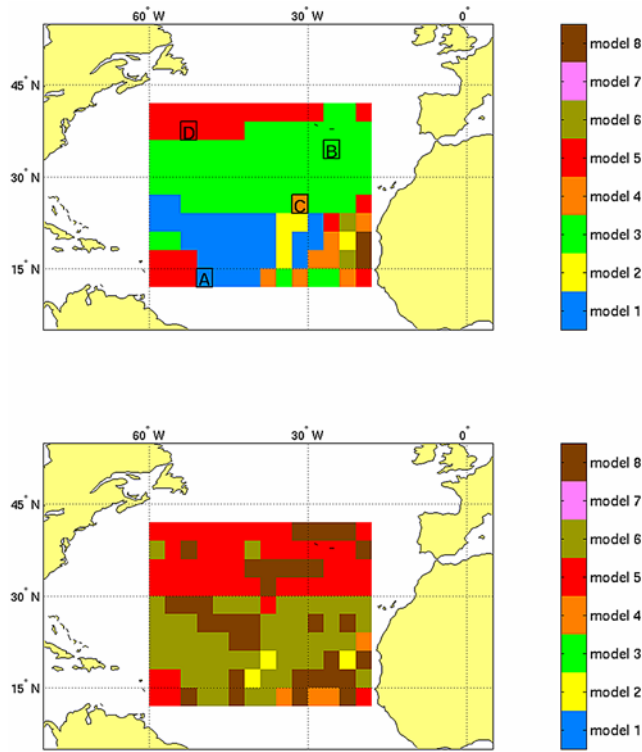[2]Cooperative Institute for Climate Studies, University of Maryland, College Park, Maryland, USA.

Figure 1. Study area (North Atlantic 42°N–15°N, 60°W–21°W) showing the spatial distribution of fitted models; each color represents a different model. (Top) Results from the Gamma GLM approach. (Bottom) Results from the OLS linear regression approach. Letters A, B, C, and D represent regions where annual cycles of chlorophyll concentration are described by statistical models 1, 3, 4, and 5, respectively (Table 1).

consequence is the prediction of unphysical non-negative values and confidence intervals including negative values. Arguably less noticeable (but more important for climate studies), hypothesis testing based on the Gaussian distribution is flawed when the data are non-Gaussian and p-values (or other such statistics) can be misleading or inaccurate. This issue is often best shown by considering common residual diagnostics but is shown here by comparison of our results with those obtained using a similar forward model selection technique for Ordinary Least Squares (OLS) linear regression.

[7] For these reasons, the time series of chlorophyll Y at each grid box in the study area was modeled using a Gamma Generalized Linear Model (GLM) with the canonical log link:

$$Y|\eta \sim \text{Gamma}(\mu, \nu)$$
$$\log(\mu) = \eta = \beta_0 + \beta_1 x_1 + \ldots + \beta_j x_j + \ldots + \beta_p x_p$$

where μ is the mean chlorophyll concentration, η is the model applied, ν is the shape parameter of the Gamma distribution, x_j is the jth explanatory variable and β_j are the regression parameters. GLMs are a powerful regression tool which allow for modeling and hypothesis testing for a range of non-Gaussian distributions [McCullagh and Nelder, 1989]. The Gamma distribution was used to model chlorophyll because of its ability to represent multiple shapes (through the estimation of a shape parameter) that include nearly symmetric distributions such as those seen in the tropics as well as highly skewed distributions common at higher latitudes in the North Atlantic. Variables were added to represent a linear time trend, the annual cycle and linear time trends in the annual cycle, i.e. the terms [$\beta_1 \times t$], [$\beta_1 \times Sin\,(2\pi t) + \beta_2 \times Cos\,(2\pi t)$], and [$\beta_4 \times Sin\,(2\pi t) \times t + \beta_5 \times Cos\,(2\pi t) \times t$], respectively, in Table 1). First and second order sinusoidal shapes were used to represent the annual cycle. For the OLS linear regression comparison, the same forward selection strategy was used where the term which explained the most sums of squares was added to the model at each step. In this case, F-tests were used to assess the statistical significance of the term to be added.

[8] Dates of bloom onset, maturity, start of bloom decay, and bloom termination were extracted from the fitted functions using the criteria of Jonsson and Eklundh [2004]. Using minimum and maximum concentrations established from the fitted model over the annual cycle at a given location, bloom onset and termination are defined as

from SeaWiFS Level 3 Binned (version 5.2) files. This area was chosen due to its well-described seasonal patterns in phytoplankton biomass and the relative heterogeneity in the form of the annual cycle across the basin. The time period examined includes strong El Niño (1997–98) and La Niña (1998–99) events.

[6] The distribution of chlorophyll can be highly non-Gaussian and methods based on the assumption of Gaussian distributed residuals (such as ordinary least squares linear regression) are generally inadequate. The most obvious

Table 1. Nested Statistical Models Used in the Study to Describe the Annual Cycle of Chlorophyll Concentration in the Central North Atlantic

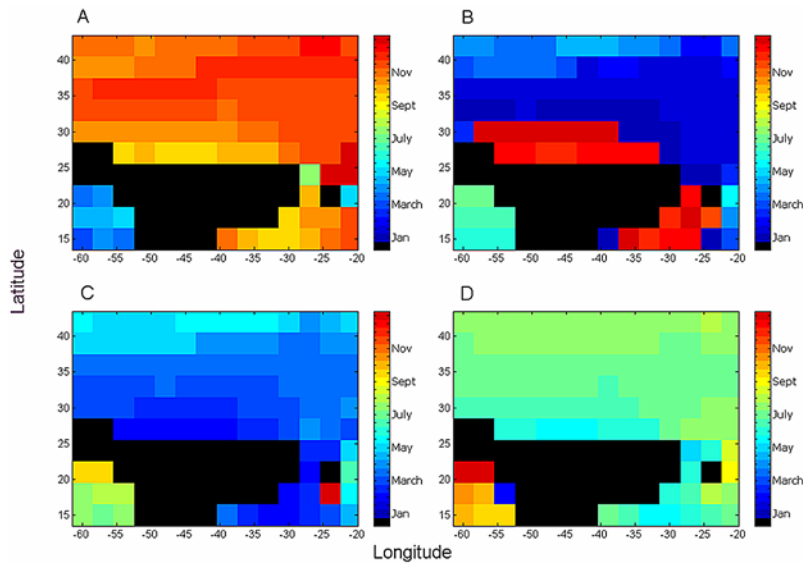| Model Number	Fitted Models
1	$\log(\mu) = \beta_0$
2	$\log(\mu) = \beta_0 + [\beta_1 \times t]$
3	$\log(\mu) = \beta_0 + [\beta_2 \times Sin(2\pi t) + \beta_3 \times Cos(2\pi t)]$
4	$\log(\mu) = \beta_0 + [\beta_1 \times t] + [\beta_2 \times Sin(2\pi t) + \beta_3 \times Cos(2\pi t)]$
5	$\log(\mu) = \beta_0 + [\beta_2 \times Sin(2\pi t) + \beta_3 \times Cos(2\pi t)] + [\beta_4 \times Sin(4\pi t) + \beta_5 \times Cos(4\pi t)]$
6	$\log(\mu) = \beta_0 + [\beta_1 \times t] + [\beta_2 \times Sin(2\pi t) + \beta_3 \times Cos(2\pi t)] + [\beta_4 \times Sin(4\pi t) + \beta_5 \times Cos(4\pi t)]$
7	$\log(\mu) = \beta_0 + [\beta_1 \times t] + [\beta_2 \times Sin(2\pi t) + \beta_3 \times Cos(2\pi t)] + [\beta_6 \times Sin(2\pi t) \times t + \beta_7 \times Cos(2\pi t) \times t]$
8	$\log(\mu) = \beta_0 + [\beta_1 \times t] + [\beta_2 \times Sin(2\pi t) + \beta_3 \times Cos(2\pi t)] + [\beta_4 \times Sin(4\pi t) + \beta_5 \times Cos(4\pi t)] + [\beta_6 \times Sin(2\pi t) \times t + \beta_7 \times Cos(2\pi t) \times t]$

Figure 2. Spatial distribution of (a) bloom onset, (b) bloom maturity, (c) start of bloom decay, and (d) bloom termination.

the period when chlorophyll concentration attains and declines, respectively, to 10% of the maximum concentration. Similarly, bloom maturity and decay are defined as the period when chlorophyll concentration attains and declines, respectively, to 90% of the maximum concentration observed over the annual cycle.

3. Results

[9] Figure 1 (top) shows the spatial distribution of the eight models constructed to represent the annual cycle of chlorophyll concentration in the study area, with each color representing a different statistical model listed in Table 1. Figure 1 (bottom) shows similar results obtained using OLS linear regression. There are stark differences between the two analyses, with the OLS linear regression approach tending to choose higher order models such as models 5 and 6. This is a consequence of the model inadequacy: the OLS linear regression approach frequently chooses models with the second harmonic or a time trend, where neither is needed. This example illustrates the perils of using simple Gaussian techniques for non-Gaussian data. While incorrectly specified models might provide an adequate functional form, statistical inference based on such models is usually unreliable and can lead to misleading results such as spurious trends.

[10] The GLM results (Figure 1, top) show clusters of pixels with the same color that share similar bloom dynamics. For example, blue pixels (model 1) denote the locations where no trend and no statistically significant annual cycle in chlorophyll concentrations were found. Green pixels (model 3) indicate the locations where a stationary, first order annual cycle exists. Orange pixels (model 4) signify the sites where both a stationary first order annual cycle and a decreasing linear trend in chlorophyll concentration over the nine-year period were detected. The red pixels (model 5) represent the positions where a stationary second order annual cycle was observed. These areas exhibit a clear annual cycle in chlorophyll, including a major peak in April

and a minor peak in October, requiring a second order sinusoidal model to capture the more complex structure of the chlorophyll time series. The minor peak of chlorophyll in October is followed only by a minimal decrease and then continues to increase to the April maximum.

[11] Models 3, 1, and 5 are the most frequent models in the study area, creating coherent, homogeneous structures that are predominately found in the open ocean and zonally distributed. The remaining, less numerous models are observed closer to land and in the southernmost latitudes of the study area, and form a diverse mosaic (Figure 1, top). Models 3 to 8 characterize regions with consistent annual cycles of growth and decay.

[12] The spatial distributions of average bloom onset, maturity, start of bloom decay and bloom demise over the nine years analyzed are illustrated in Figure 2. Above 24°N, blooms begin in autumn (September – November), reach maturity in late autumn to winter (December – February), start to decay in spring (March – May) and terminate during summer (June – August). The timing of the markers is similar for surface waters in the southeastern portion of the study area off Africa, yet occurs up to six months earlier in waters comprising the southwestern portion of the study area off South America. The phenological markers cannot be determined for a large region in the southern portion of the study area because it does not possess a statistically significant annual cycle. In this region, the mean represents the best estimate to describe its concentration at any given time. The general meridional pattern of timing of all phenological markers in the open ocean and southeastern portion of the study area is also evident, with the timing of each marker occurring later at higher latitudes (Figure 2).

[13] No statistically significant trends in the timing of the phenological markers could be detected. The number of years available was insufficient to clearly distinguish a signal from the noise. However, decreasing linear trends in the magnitudes of chlorophyll concentration were observed in regions fitted to Models 2, 4, 6, 7 and 8 (Figure 1, top). For instance, the annual chlorophyll

concentration coincident with bloom maturity at location C declined approximately 0.04 mg m^{-3} over the nine-year period.

4. Discussion

[14] The phenological results extracted from the Generalized Linear Models (GLM) of SeaWiFS chlorophyll concentrations in this study generally agree and are consistent with the shape and timing of the annual cycle of phytoplankton biomass in the North Atlantic as conceived by [*Cushing*, 1959] and observed by others [*Follows and Dutkiewicz*, 2002; *Siegel et al.*, 2002; *Ueyama and Monger*, 2005]. Models displaying single annual cycles of chlorophyll concentration, with and without secondary peaks, were found in the temperate to southern subpolar waters in homogenous groupings in a zonal pattern (Figure 1, top). Clearly defined blooms were absent in open ocean waters at subtropical latitudes. Bloom onset, the only marker for which information is available for comparison, began in autumn (Figure 2a). This result is similar to or somewhat earlier than the periods (October to January) reported by others [*Ueyama and Monger*, 2005; *Siegel et al.*, 2002]. Any discrepancies likely reflect the different methodologies in modeling the chlorophyll concentrations and the criteria applied in defining the phenological markers employed by the various studies. Our criterion for bloom onset – the period when chlorophyll concentration increases to 10% of the annual maximum – would be expected to yield an earlier date than that used by *Siegel et al.* [2002] – the date when chlorophyll attains an abundance of 5% greater than the annual median concentration.

[15] No statistically significant annual cycle was detected in the southern portion of the subtropical gyre, suggesting either a weak annual cycle (not detectable against the noise in the remotely sensed data) or no actual annual cycle. This result is analogous to that obtained by *Henson and Thomas* [2007], who encountered difficulties in determining bloom onset in regions with weak seasonality, yet contrasts with *Ueyama and Monger* [2005] where they were able to extract bloom onset (and end date) using a least-squares fitting approach.

[16] The decreasing linear trends of chlorophyll concentration detected in the southeastern portion of our study area off Africa (Figure 1, top) agrees with the general decreasing trend of chlorophyll concentration anomalies found in low-latitude, permanently stratified waters over the same period [*Behrenfeld et al.*, 2006] and suggests these decreases are restricted to certain regions in these latitudes. A statistically significant decreasing trend in chlorophyll concentration was not detected, however, to the east of the Lesser Antilles where *Polovina et al.* [2008] observed a rapid expansion in the surface area of waters possessing chlorophyll concentrations not exceeding 0.07 mg chl/m^3, and consequently lower average chlorophyll concentration, during the months of December over the same period as this study. The reason for this discrepancy is not clear and requires further inquiry.

[17] We have shown that OLS linear regression can lead to misleading results for non-Gaussian data and used an existing regression-like approach to correctly model the distribution of chlorophyll concentrations. This novel approach of statistically modeling the time series of phytoplankton biomass has allowed us to document and analyze the interannual variability and short-term trends of bloom onset, maturity, decay and termination in the central North Atlantic. The next logical step for this work is to extend the approach globally so as to construct climatologies of these phenological markers for all oceanic regions that can be used to assess the temporal response in the annual cycle of phytoplankton biomass and gain a better understanding of the response of marine ecosystems to climate change. Additionally, several modifications to the technique might help to reduce the residual noise such as a more flexible model for the annual cycle or the inclusion of other explanatory variables (e.g. SST) to account for unrelated noise.

References

Beaubien, E. G., and M. Hall-Beyer (2003), Plant phenology in western Canada: Trends and links to the view from space, *Environ. Monit. Assess.*, *88*, 419–429.

Behrenfeld, M. J., et al. (2001), Biospheric primary production during an ENSO transition, *Science*, *291*, 2594–2597.

Behrenfeld, M. J., R. T. O'Malley, D. A. Siegel, C. R. McClain, J. L. Sarmiento, G. C. Feldman, A. J. Milligan, P. G. Falkowski, R. M. Letelier, and E. S. Boss (2006), Climate-driven trends in contemporary ocean productivity, *Nature*, *444*, 752–755.

Cushing, D. H. (1959), The seasonal variation in oceanic production as a problem in phytoplankton dynamics, *J. Cons. Int. Explor. Mer.*, *24*, 455–464.

Delbart, N., T. Le Toan, L. Kergoat, and V. Fedotova (2006), Remote sensing of spring phenology in boreal regions: A free of snow-effect method using NOAA-AVHRR and SPOT-VGT data (1982–2004), *Remote Sens. Environ.*, *101*, 52–62.

Edwards, M., and A. J. Richardson (2004), Impact of climate change on marine pelagic phenology and trophic mismatch, *Nature*, *430*, 881–884.

Follows, M., and S. Dutkiewicz (2002), Meteorological modulation of the North Atlantic spring bloom, *Deep Sea Res., Part II*, *49*, 321–344.

Gregg, W. W., and M. E. Conkright (2002), Decadal changes in global ocean chlorophyll, *Geophys. Res. Lett.*, *29*(15), 1730, doi:10.1029/2002GL014689.

Gregg, W. W., M. E. Conkright, P. Ginoux, J. E. O'Reilly, and N. W. Casey (2003), Ocean primary production and climate: Global decadal changes, *Geophys. Res. Lett.*, *30*(15), 1809, doi:10.1029/2003GL016889.

Hays, G. C., A. J. Richardson, and C. Robinson (2005), Climate change and marine plankton, *Trends Ecol. Evol.*, *20*, 337–344.

Henson, S. A., and A. C. Thomas (2007), Interannual variability in timing of bloom initiation in the California Current System, *J. Geophys. Res.*, *112*, C08007, doi:10.1029/2006JC003960.

Henson, S., I. S. Robinson, J. T. Allen, and J. J. Waniek (2006), Effect of meteorological conditions on interannual variability in timing and magnitude of the spring bloom in the Irminger Basin, North Atlantic, *Deep Sea Res., Part I*, *53*, 1601–1615.

Jonsson, P., and L. Eklundh (2004), TIMESAT: A program for analyzing time-series of satellite sensor data, *Comput. Geosci.*, *30*, 833–845.

McCullagh, P., and J. A. Nelder (1989), *Generalized Linear Models*, 2nd ed., Chapman and Hall, London.

Myneni, R. B., C. D. Keeling, C. J. Tucker, G. Asrar, and R. R. Nemani (1997), Increased plant growth in the northern high latitudes from 1981 to 1991, *Nature*, *386*, 698–702.

Platt, T., C. Fuentes-Yaco, and K. T. Frank (2003), Spring algal bloom and larval fish survival, *Nature*, *423*, 398–399.

Polovina, J. J., E. A. Howell, and M. Abecassis (2008), Ocean's least productive waters are expanding, *Geophys. Res. Lett.*, *35*, L03618, doi:10.1029/2007GL031745.

Sarmiento, J. L., et al. (2004), Response of ocean ecosystems to climate warming, *Global Biogeochem. Cycles*, *18*, GB3003, doi:10.1029/2003GB002134.

Schwartz, M. D. (1999), Advancing to full bloom: Planning phenological research for the 21st century, *Int. J. Biometeorol.*, *42*, 113–118.

Siegel, D. A., S. C. Doney, and J. A. Yoder (2002), The North Atlantic spring phytoplankton bloom and Sverdrup's critical depth hypothesis, *Science*, *296*, 730–733.

Stenseth, N. C., and A. Mysterud (2002), Climate, changing phenology, and other life history traits: Nonlinearity and match-mismatch to the environment, *Proc. Natl. Acad. Sci. U. S. A.*, *99*, 13,379–13,381.

Ueyama, R., and B. C. Monger (2005), Wind-induced modulation of seasonal phytoplankton blooms in the North Atlantic derived from satellite observations, *Limnol. Oceanogr.*, *50*, 1820–1829.

Yoder, J. A., C. R. McClain, G. C. Feldman, and W. E. Esaias (1993), Annual cycles of phytoplankton chlorophyll concentrations in the global ocean: A satellite view, *Global Biogeochem. Cycles*, *7*, 181–194.

Zhang, X., M. A. Friedl, and C. B. Schaaf (2006), Global vegetation phenology from Moderate Resolution Imaging Spectroradiometer (MODIS): Evaluation of global patterns and comparison with in situ measurements, *J. Geophys. Res.*, *111*, G04017, doi:10.1029/2006JG000217.

—————————————

C. W. Brown and M. R. P. Sapiano, Cooperative Institute for Climate Studies, University of Maryland, College Park, MD 20742, USA.

M. Vargas, NOAA/NESDIS/STAR, 5200 Auth Road Suite 712, Camp Springs, MD 20746, USA. (marco.vargas@noaa.gov)